Supplementary material to "Transcriptional correlates of the pathological phenotype in a Huntington's disease mouse model"

Andrea Gallardo-Orihuela, Irati Hervás-Corpión, Carmen Hierro-Bujalance, Daniel Sanchez-Sotano, Gema Jiménez-Gómez, Francisco Mora-López, Antonio Campos-Caro, Monica Garcia-Alloza, Luis M. Valor

Supplementary Figure S1. Phenotypical and gene expression variations across mouse cohorts. Distribution of mouse litter assignation in the plots of Fig. 2B and C. Orange, cohort 1; pink, cohort 2; green, cohort 3.

Supplementary Figure S2. Analysis of the transcription factor NF-Y in the R6/1 strain. *A*, RT-qPCR assays of cortical and striatal samples of R6/1 mice and their wild-type littermates showed a progressive reduction in *Nfya* levels, whereas the levels of *Nfyb* were unaltered; n = 7 for wild-type and n = 5 for R6/1. *B*, In contrast, Western blot assays showed a specific increase in the protein levels of NF-Y_A (normalized to histone H3 levels); n = 6 for wild-type and n = 5 for R6/1. *C*, While *Nfya* was upregulated, the NF-Y target gene *Hsp90b1* (also known as *Grp94*) was downregulated; n = 24 for wild-type and n = 29 for R6/1. *D*, The binding of NF-Y to the CCAAT box of its target genes (e.g., *Hsp90b1*) was not altered in the brains of R6/1 mice compared to the brains of their wild-type littermates. The results from the cortex and striatum are pooled; n = 4 pools of 3-4 animals per genotype. The data are expressed as mean ± s.e.m. *, $P<0.05$; **, $P<0.005$; Mann Whitney U-test.

Supplementary Figure S3. Markers of worse HD phenotype do not necessarily correlate with specific HD phenotypical traits. Upper panel, the expression of phenotype-related genes, namely *Gabrd* (gamma-aminobutyric acid type A receptor delta subunit), *Scn4b* (sodium voltage-gated channel beta subunit 4), *Pde10a* (phosphodiesterase 10A), *Tac1* (tachykinin precursor 1), *Mbd2* (methyl-CpG binding domain protein 2), *Nfya* (nuclear transcription factor Y subunit alpha), and *Trpc4* (transient receptor potential cation channel subfamily C member 4), across the four groups of animals (n = 4 each group). §, $P<0.05$ between R6/1 “poor” and “good” animals; Mann Whitney U-test. The data are expressed as the mean ± s.d. Lower panel, summary of the Spearman coefficient values showing the correlation between

phenotypical traits and gene expression levels (n = 29). Significant correlations (unadjusted $P< 0.05$; linear regression t-test) between *Gabrd* and rotarod performance.

Supplementary Figure S4. Predictive analysis of transcription binding sites. Lists of DNA motifs ($P<0.05$, Pscan) that were specifically enriched in each subset of genes associated with the R6/1 phenotype.

Supplementary Figure S1. Phenotypical and gene expression variations across mouse cohorts

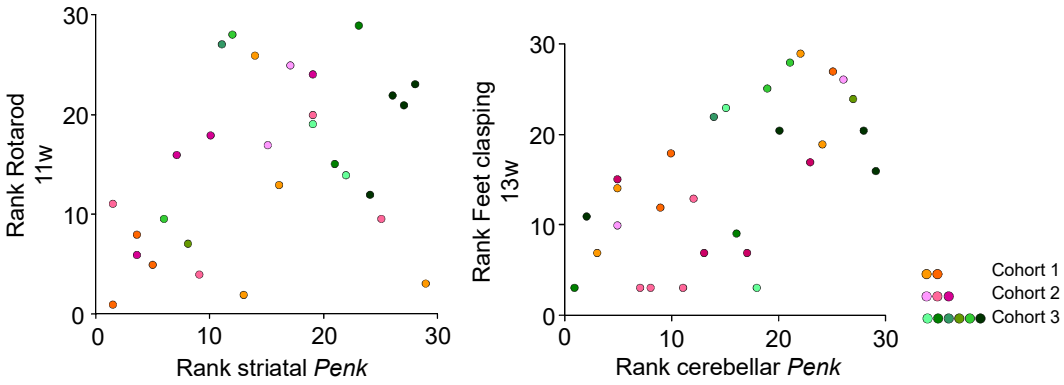

Supplementary Figure S2. Analysis of the transcription factor NF-Y in the R6/1 strain

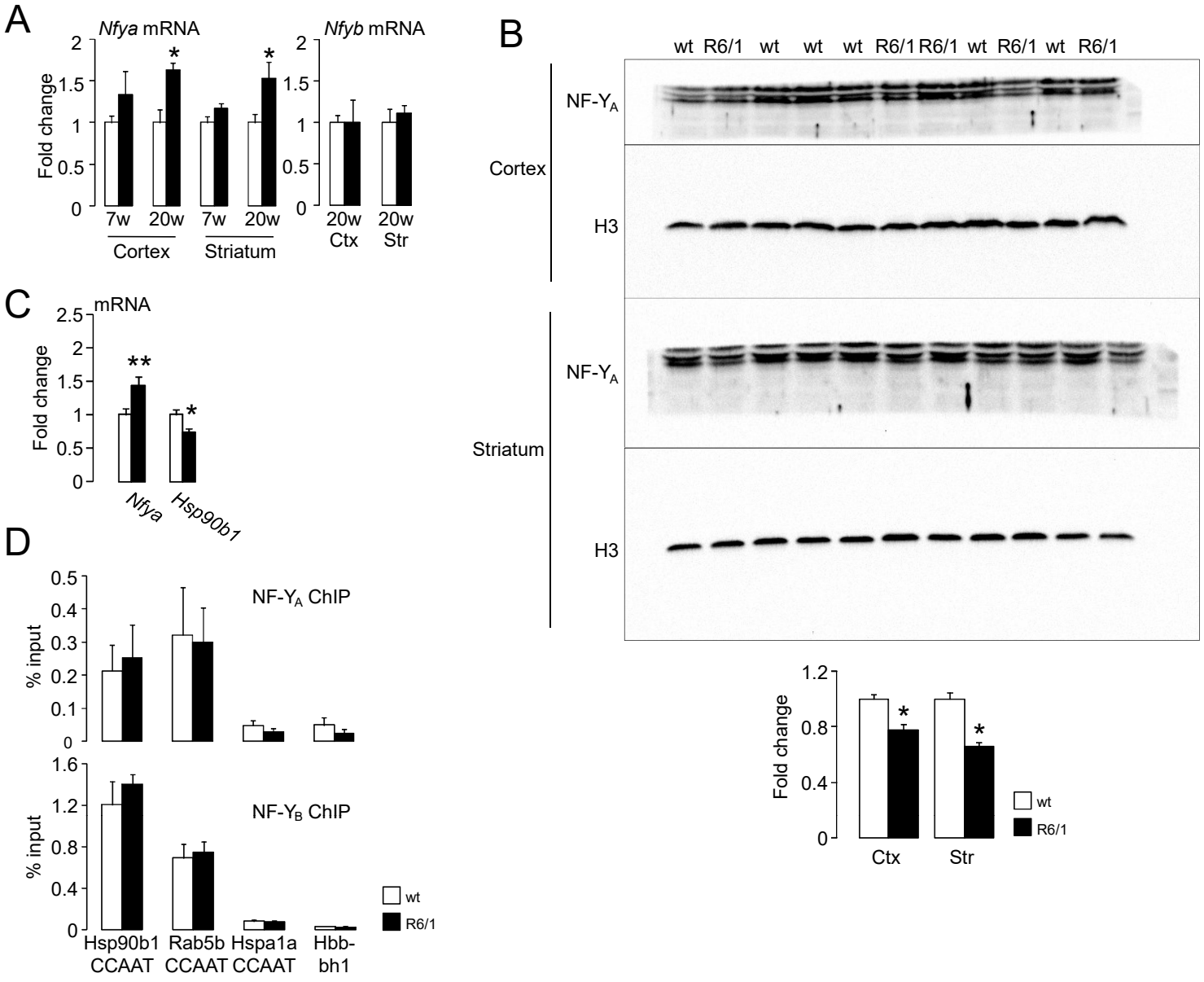

Supplementary Figure S3. Markers of worse HD phenotype do not necessarily correlate with specific HD phenotypical traits

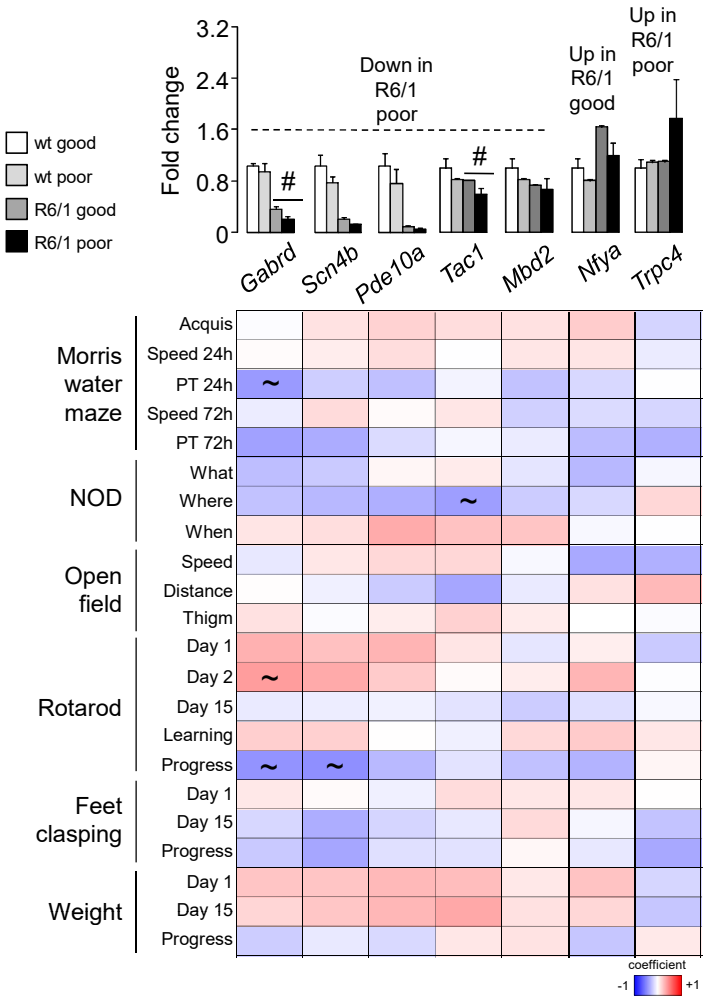

Supplementary Figure S4. Predictive analysis of transcription factor binding sites